Electrochemistry Communications 128 (2021) 107070

Contents lists available at ScienceDirect

Electrochemistry Communications

journal homepage: www.elsevier.com/locate/elecom

Thermal and electrochemical reduction of zinc ferrite doped with polymer

Nina M. Ivanova [a,*], Zainulla Muldakhmetov [a], Yakha A. Vissurkhanova [a,b], Elena A. Soboleva [a], Moldyr E. Beisenbekova [a]

[a] Institute of Organic Synthesis and Chemistry of Coal of Kazakhstan Republic, Alikhanov Str., 1, Karaganda, 100000, Kazakhstan
[b] Karaganda University named E.A. Buketov, Universitetskaya Str., 1, Karaganda 100028, Kazakhstan

ARTICLE INFO

Keywords:
Zinc (II) ferrite
Polyvinyl alcohol
Thermal and electrochemical reduction
Electrocatalytic activity

ABSTRACT

Zinc ferrite samples were prepared by a co-precipitation method in the presence and absence of a polymer stabilizer (polyvinyl alcohol), followed by heat treatment at 500, 700, and 900 °C. The structural phase and morphological features of these samples were studied by X-ray phase analysis and electron microscopy. It was found that polymer-doped zinc ferrite undergoes thermal reduction by the decomposition products of the polymer, and is also capable of further electrochemical reduction on a Cu cathode in an aqueous alkaline solution. Zinc ferrite reduction products (ZnO, Fe^0) exhibit electrocatalytic activity for the electrohydrogenation of *p*-nitroaniline.

1. Introduction

Zinc (II) ferrite ($ZnFe_2O_4$) belongs to the class of soft magnetic materials, which are characterized by properties such as chemical stability, non-toxicity, mechanical hardness, excellent electromagnetic characteristics, low coercivity and moderate saturation magnetization [1–3].

Various methods for zinc ferrite production are reported in the literature, including thermal methods, co-precipitation methods, solution combustion methods using different types of organic fuels, sol–gel approaches, hydrothermal methods, and electrochemical synthesis, among others [4–9]. Depending on the method and the conditions, it is possible to synthesize 1D, 2D, and 3D nanocrystals of $ZnFe_2O_4$ [10], as well as more complex morphological forms, such as coral-like structures [11], porous nanoparticles [12] and nanoparticles with a core–shell composition [13].

The preparation of zinc ferrite samples in the presence of polymers (PVA, PVP and PEG) to stabilize the particles and prevent them from agglomeration has also been described [6,14–16]. In these reports, the effect of polymer stabilizers on the optical, magnetic, structural and other properties of zinc ferrite was studied. As a rule, the reaction mixture comprising the polymer with metal salts (or their hydroxides) was subjected to evaporation prior to calcination.

Zinc ferrite is a commercially important material. It can be used as the anode in lithium-ion batteries, in sensors, as a sorbent for heavy metal cations, in photocatalysis and catalysis of important chemical processes, in medicine, etc. [6,17–21]. Zinc ferrite is also an important component of the dust from electric arc furnaces, which is formed as a waste product of steel production. This dust contains large amounts of zinc and iron and is a secondary raw material for their production. One of the methods developed for extraction of the metals [22,23] is thermal recovery of the dust in a stream of reducing gases (CO, CO_2, H_2). According to the reports [24–27], the reduction of $ZnFe_2O_4$ by CO-N_2 and CO-CO_2 gas mixtures in the temperature range 800–1100 °C is accompanied by the formation of ZnO, FeO, Fe_3O_4, Fe and Zn products.

In our recent study [28], it was found that thermally treated copper (II) ferrite synthesized without polymer stabilizers can be reduced in an electrochemical system with the formation of one or two reduced metals, depending on the temperature of heat treatment of the $CuFe_2O_4$ samples. $Cu_{0.5}Ni_{0.5}Fe_2O_4$ and $NiFe_2O_4$ ferrites exhibit this behaviour only if they are doped with a polymer [29,30]. In this paper, the possibility of thermal and electrochemical reduction (ECR) of zinc ferrite ($ZnFe_2O_4$) under the influence of a polymer additive (polyvinyl alcohol (PVA)) is reported. The phase compositions of the resulting iron- and zinc-containing products and their electrocatalytic activity for the electrohydrogenation (EH) of *p*-nitroaniline (*p*-NA) as a model compound are determined.

2. Experimental

The zinc ferrite was synthesized using a co-precipitation synthetic

* Corresponding author.
E-mail address: nmiva@mail.ru (N.M. Ivanova).

https://doi.org/10.1016/j.elecom.2021.107070
Received 12 May 2021; Received in revised form 27 May 2021; Accepted 2 June 2021
Available online 5 June 2021

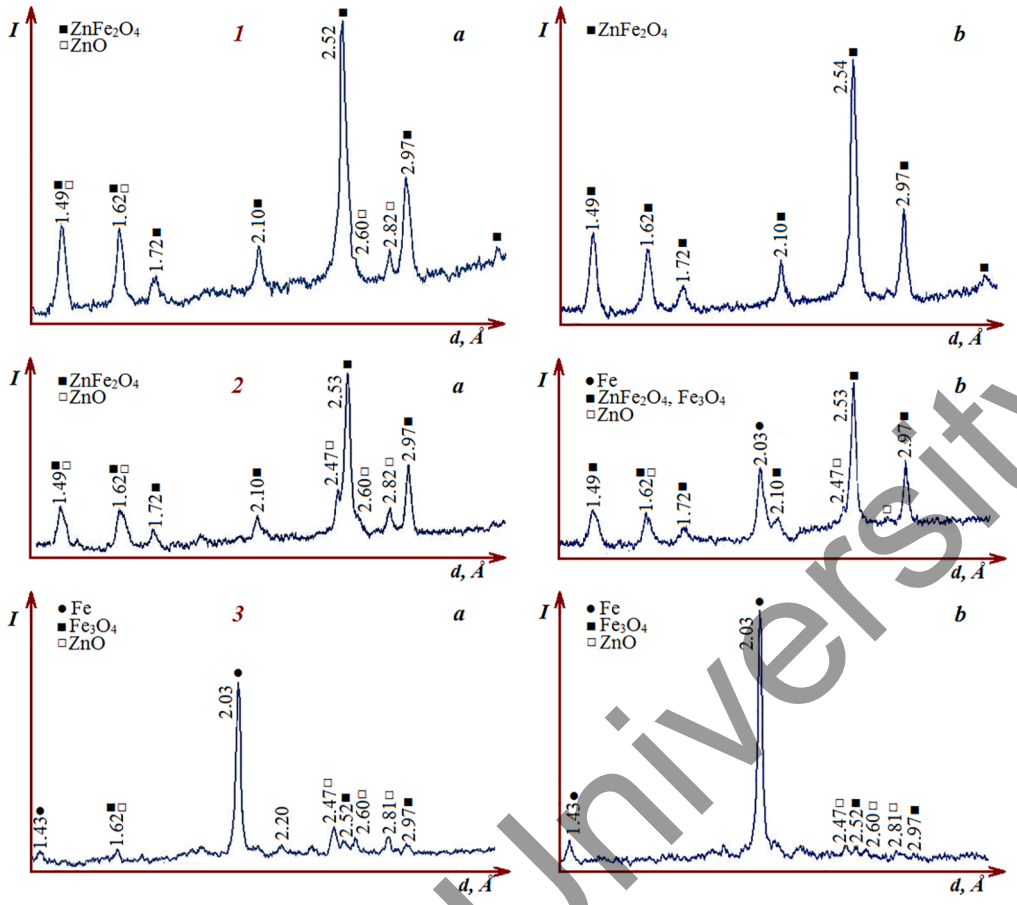

Fig. 1. XRD patterns of $ZnFe_2O_4$ + PVA ((1) 500 °C, (2) 700 °C, (3) 900 °C) samples (*a*) after heat treatment and (*b*) after EH of *p*-NA.

route described elsewhere [28–30]. Briefly, $Zn(NO_3)_2{\cdot}6H_2O$ (0.06 mol) and $Fe(NO_3)_3{\cdot}9H_2O$ (0.12 mol) salts were dissolved in distilled water and stirred with a magnetic stirrer at 40 °C for 30 min. A 2 M NaOH solution was added dropwise to the mixture with constant stirring to obtain pH 12. A dark brown precipitate was gradually formed. The precipitate was filtered and washed with distilled water, heated to 50 °C, and dried at 80 °C to constant weight. The prepared powder was divided into three equal parts and heat treated in closed crucibles at 500 °C, 700 °C and 900 °C for 2 h.

To produce zinc ferrite doped with PVA polymer, the samples were prepared using the above-described synthetic route but with dissolution of the zinc and iron salts in 3% PVA solution before adjusting the pH to 12. The resulting precipitate was centrifuged, washed with distilled water of room temperature and filtered. After drying, the $ZnFe_2O_4$ + PVA samples were also subjected to heat treatment (HT).

The X-ray diffraction (XRD) analysis of the zinc ferrite samples after heat treatment and electrochemical experiments was performed on a DRON-2 diffractometer using Cu Kα radiation. Scanning electron microscopy (SEM) studies of the morphologies of the samples were conducted with a TESCAN MIRA 3LMU microscope. The elemental compositions of the samples were identified using X-ray spectral analysis (or energy dispersive spectroscopy (EDS)).

In the first stage of the electrochemical experiments, the reduction of previously heat-treated $ZnFe_2O_4$ samples was carried out in a diaphragm cell in an aqueous alkaline solution (the initial concentration was 2% NaOH) using a current of 1.5 A and a temperature of 30 °C. A Pt gauze served as an anode. The zinc ferrite powder (1 g) was deposited on a horizontally located Cu cathode with a surface area of 0.05 dm^2, which fitted closely to the bottom of the cell. The $ZnFe_2O_4$ powders that have magnetic properties could be held on the cathode surface by an external magnet placed beneath the electrolyzer.

Electrocatalytic hydrogenation (ECH) of *p*-NA using the reduced metal composites as catalysts (the second stage) was carried out after the termination of hydrogen absorption in the first stage. The *p*-NA dissolved in ethanol was added to the catholyte in the ratio 1:2 with respect to the alkaline catholyte solution. The *p*-NA concentration in the catholyte was 0.066 M. Electrohydrogenation of *p*-NA was carried out using a current of 1.5 A and a temperature of 30 °C.

3. Results and discussion

3.1. Structural phase changes

The XRD analysis of the powder after the co-precipitation procedure shows the existing zinc oxide and, possibly, weakly crystallized iron (III) hydroxide. The phase constitution of the powder heat-treated at 500 °C, 700 °C and 900 °C is represented only by crystalline phases of zinc ferrite with a spinel structure, the crystallinity of which rises with the increase in the HT temperature. Attempts to reduce the prepared zinc ferrite samples in an electrochemical system were unsuccessful. Zinc ferrite is not reduced under the same conditions as copper ferrite [27]. Furthermore, after experiments involving the EH of *p*-NA, the phase constitutions of all three samples turned out to be the same as after the heat treatment.

The changes in the structural phases of samples of zinc ferrite synthesized in the presence of PVA under the action of the products of thermal decomposition of the polymer, as well as after the electrochemical experiments, are illustrated by the XRD patterns shown in Fig. 1.

The sample of $ZnFe_2O_4$ + PVA thermally treated at 500 °C (Fig. 1, 1a) contains crystalline phases of zinc ferrite and a small amount of zinc oxide. The $ZnFe_2O_4$ + PVA (700 °C) sample has a similar phase

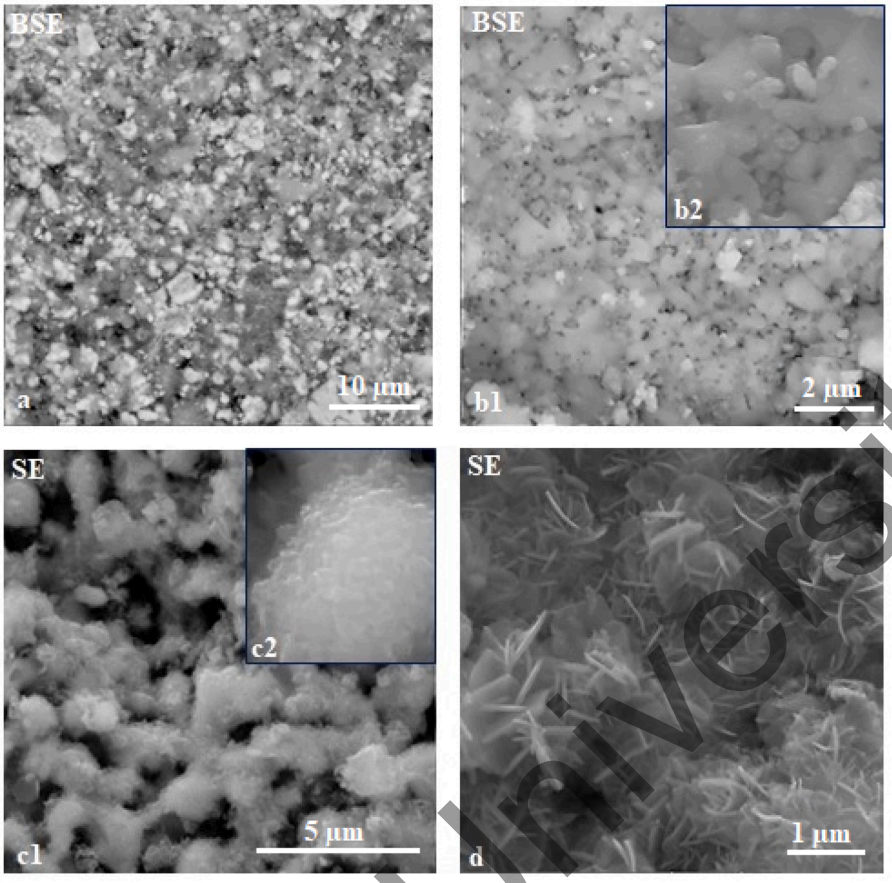

Fig. 2. Micrographs of the particles (*a*) in the $ZnFe_2O_4$ + PVA (700 °C) sample after HT; (*b*) in the $ZnFe_2O_4$ + PVA (700 °C) sample and (*c,d*) in the $ZnFe_2O_4$ + PVA (900 °C) sample after EH of *p*-NA. These were produced using BSE and SE electron detectors.

constitution (Fig. 1, 2a). Magnetite (Fe_3O_4) formed in small amounts has the same interplanar distances in the crystallites as zinc ferrite, and its corresponding peaks are not visible in the XRD patterns. The $ZnFe_2O_4$ + PVA (900 °C) sample is represented mainly by crystalline phases of reduced iron with a small amount of zinc oxide, the remainder being magnetite (Fig. 1, 3a). The absence of the crystalline phases of reduced zinc and the low content of ZnO in this sample are explained by the evaporation of zinc accompanying heat treatment at 900 °C, which has also been noted in papers about $ZnFe_2O_4$ reduction with gases [24–27]. In our experiments, a white precipitate found on the crucible lid after heat treatment corresponded to ZnO, according to XRD analysis.

The XRD patterns of $ZnFe_2O_4$ + PVA samples recorded after their ECR and ECH of *p*-NA (Fig. 1, 1b-3b) also demonstrate differences in composition depending on the temperature of the heat treatment. The phase constitution of the $ZnFe_2O_4$ + PVA (500 °C) sample (Fig. 1, 1b) is almost the same as its thermally treated precursor, and is characterized only by a decrease in the ZnO content, which was partially transferred to the catholyte solution. The presence of zinc cations in the catholyte and the observed weak zinc-plating of the cathode surface were confirmed by the atomic emission spectral analyses. In the phase constitution of the $ZnFe_2O_4$ + PVA (700 °C) sample after the electrochemical experiments (Fig. 1, 2b), crystalline phases of electrochemically reduced iron appear, together with, obviously, Fe_3O_4 with residues of $ZnFe_2O_4$, as well as small amounts of ZnO. In the electrochemical cell, the $ZnFe_2O_4$ + PVA (900 °C) sample undergoes additional and almost complete reduction. This sample contains mainly crystalline phases of reduced iron with small amounts of ZnO and Fe_3O_4 as impurities (Fig. 1, 3b).

According to the SEM studies, the size of the zinc ferrite grains rises with increasing HT temperature and decreases when the polymer is present. So, the grain sizes in the $ZnFe_2O_4$ (700 °C) sample are mainly ~60–120 nm, and they are collected in agglomerated particles. In the $ZnFe_2O_4$ + PVA (700 °C) sample, the grains are smaller (~40–90 nm), but they are also combined into large particles.

Micrographs of some $ZnFe_2O_4$ + PVA samples are shown in Fig. 2. These micrographs were taken using two detectors: the SE (secondary electrons) and the BSE (back-scattered electrons) detectors, which make it possible to obtain images with topographic contrast and compositional variations, respectively.

On the surface of particles in a $ZnFe_2O_4$ + PVA (700 °C) sample after heat treatment (Fig. 2, a) there are light and dark formations with different compositions of chemical elements. According to EDS analysis, these are elements Fe, O, Zn, Na. Here, particles with a predominant content of ZnO and Fe_3O_4 are lighter in colour. In the same sample after experiments in an electrochemical cell, in which zero-valent iron appears as a result of electrochemical reduction (Fig. 1, 2b), there are formations with the shape of a torus (or a donut with a hole in the middle) (Fig. 2, b1 and b2). In this micrograph, the lighter-colored particles are iron crystallites. The toroidal formations are composed of the elements Fe (50–62%), O (20–38%), Zn (12–15%), obviously in the form of Fe_3O_4 with a smaller amount of $ZnFe_2O_4$.

With a more complete reduction of zinc ferrite in the $ZnFe_2O_4$ + PVA (900 °C) sample, the opening of the toroidal structures occurs with the formation of serpentine and interconnected structures of reduced iron at the smallest scale (Fig. 2, c2). It is possible that these layered formations of iron are an intermediate building material for the formation of larger crystallites of iron in the form of plates and twigs, which are also present in this sample after electrochemical experiments have been completed (Fig. 2, d).

Table 1
Results obtained for the electrochemical reduction of zinc ferrite samples and the electrocatalytic hydrogenation of *p*-NA in their presence.

Zinc ferrite samples	Electrochemical reduction of zinc ferrite		Electrocatalytic hydrogenation of *p*-NA					
	τ, min	V_{H2}, mL	*W*, mL H_2/min (α = 0.25)	*α*, %	Faradaic efficiency for various α, %			
					0.25	0.50	0.75	α_{final}
Cu cathode	–	–	6.6	89.5	–	–	–	–
$ZnFe_2O_4$ (500 °C)	20	11.4	2.6	75.2	25.9	20.4	12.0	–
$ZnFe_2O_4$ (700 °C)	10	4.3	0.0	0.0	–	–	–	–
$ZnFe_2O_4$ (900 °C)	10	4.3	0.0	0.0	–	–	–	–
$ZnFe_2O_4$ + PVA (500 °C)	10	8.7	7.5	95.3	71.8	69.2	58.0	36.5
$ZnFe_2O_4$ + PVA (700 °C)	80	105.0	8.0	99.9	76.9	73.8	68.8	31.9
$ZnFe_2O_4$ + PVA (900 °C)	20	17.2	8.2	94.5	78.2	78.1	71.9	36.2

These studies of the $ZnFe_2O_4$ samples synthesized in a PVA medium make it possible to trace the change in the crystal structure at different stages of their reduction. It can be noted that in the $ZnFe_2O_4$ + PVA (700 °C and 900 °C) samples, after the electrochemical experiments, there are structural formations with particles at various degrees of reduction and crystal formation.

3.2. Electrochemical reduction and electrocatalytic activity

The synthesized and heat-treated $ZnFe_2O_4$ samples were studied for their electrochemical reduction ability, and the resulting composites were also tested for any manifestation of electrocatalytic properties in the electrohydrogenation of *p*-nitroaniline (Table 1). For the ECR stage (where relevant) the values of the duration (τ) of the stage and volume of absorbed hydrogen (V_{H2}) are given. For the *p*-NA ECH stage, the following characteristics are indicated in Table 1: *W* is the average rate of hydrogenation over the period of *p*-NA conversion for $\alpha = 25\%$, where *α* is the degree of *p*-NA conversion, as well as the Faradaic efficiency calculated for different values of α.

The characteristics of *p*-NA hydrogenation in the presence of composites fabricated from zinc ferrite are compared with the process of electrochemical reduction on a Cu cathode under similar conditions. The process occurred at a good rate with a relatively high degree of *p*-NA conversion (Table 1), but the yield of *para*-phenylenediamine (*p*-PDA) was almost 60%.

According to the data in Table 1, the $ZnFe_2O_4$ samples prepared in the absence of polymer hardly undergo any electrochemical reduction and do not exhibit electrocatalytic activity for the EH of *p*-NA. Moreover, in their presence, the ECR of *p*-NA is slowed down or inhibited.

A different picture is observed for $ZnFe_2O_4$ samples synthesized in PVA solution. The $ZnFe_2O_4$ + PVA (700 °C) sample undergoes electrochemical reduction to a greater degree; this is accompanied by the absorption of 105 ml of H_2 (Table 1). It follows from the XRD pattern of this sample (Fig. 1, 2b), in the electrochemical stage, that additional reduction of iron cations occurs, obviously from Fe_3O_4. Since in the $ZnFe_2O_4$ + PVA (900 °C) sample zinc evaporates during heat treatment, and the iron cations are almost completely reduced (Fig. 1, 3a), only 17.2 ml H_2 is used in the reduction process in the electrochemical system. In the $ZnFe_2O_4$ + PVA (500 °C) sample, iron is not reduced, but it appears that the reduction of zinc cations from ZnO occurs to a small extent, which catalyzes the EH of *p*-NA. A more marked electrocatalytic effect is observed when using iron-containing composites formed from samples thermally treated at 700 °C and 900 °C. Compared with the ECR of *p*-NA on a Cu cathode (Table 1), both the hydrogenation rate and the conversion of *p*-NA increase. According to chromatographic analyses, the main hydrogenation product, *p*-PDA, is formed with a yield of ~ 96%. The calculated values of the Faradaic efficiency (Table 1) show a significant decrease after 75% conversion using the resulting composites.

4. Conclusions

Synthesis of zinc ferrite samples in a polymer solution (PVA) followed by (non-intensive) washing of the resulting precipitates, heat treatment and electrochemical reduction made it possible to produce Fe-Zn composites containing reduced iron with small impurities (ZnO, Fe_3O_4) and zinc oxide (by evaporation of zinc). The iron-containing composites showed good electrocatalytic activity toward the electrohydrogenation of *p*-NA. In addition, these results can serve as a basis for creating a technological method for extracting iron and zinc from the zinc ferrite contained in the dust of electric arc furnaces in metallurgical plants.

Declaration of Competing Interest

The authors declare that they have no known competing financial interests or personal relationships that could have appeared to influence the work reported in this paper.

Acknowledgements

This research is funded by the Science Committee of the Ministry of Education and Science of the Republic of Kazakhstan (Grant No. AP08855930)

References

[1] A. Pradeep, P. Priyadharsini, G. Chandrasekaran, J. Alloys Compd. 509 (2011) 3917–3923.
[2] R. Shahraki, M. Ebrahimi, S.A. Seyyed Ebrahimi, S.M. Masoudpanah, J. Magn. Magn. Mater. 324 (2012) 3762–3765.
[3] M.S. Hossain, S.M. Hoque, S.I. Liba, S.h. Choudhury, AIP Adv. 7 (2017) 105321–105327.
[4] S.O. Aisida, P.A. Akpa, I. Ahmad, M. Maaza, F.I. Ezema, Physica B 571 (2019) 130–136.
[5] M. Chithra, C.N. Anumol, B. Sahu, S.C. Sahoo, Mater. Res. Exp. 6 (2019) 2–19.
[6] X. Zhu, F. Zhang, M. Wang, J. Ding, S. Sun, J. Bao, C. Gao, Appl. Surface Sci. 319 (2014) 83–89.
[7] F. Iqbal, M.I.A. Mitalib, M.S. Shaharun, M. Khan, B. Abdullah, Procedia Eng. 148 (2016) 787–794.
[8] C. Hu, Z. Gao, X. Yang, J. Magn. Magn. Mater. 320 (2008) L70–L73.
[9] E.M. Elsayed, M.M. Rashad, H.F.Y. Khalil, I.A. Ibrahim, M.R. Hussein, M.M.B. El-Sabbah, Appl. Nanosci. 6 (2016) 485–494.
[10] V.I. Popkov, V.P. Tolstoy, V.G. Semenov, J. Alloys Compd. 813 (2020), 152179.
[11] Y. Lin, J. Zhang, M. Li, L. Wang, H. Yang, J. Alloys Compd. 726 (2017) 154–163.
[12] S. Sun, X. Yang, Y. Zhang, F. Zhang, J. Ding, J. Bao, C. Gao, Prog. Nat. Sci.: Mater. Int. 22 (2012) 639–643.
[13] J.A. Gomes, G.M. Azevedo, J. Depeyrot, J. Mestnik-Filho, F.L.O. Paula, F. A. Tourinho, R. Perzynski, J. Phys. Chem. C 116 (2012) 24281–24291.
[14] R. Sahanakumari, V. Ravindrachary, B.K. Mahantesha, R. Padmakumari, P. Tegginamata, J. Phys.: Conf. Ser. 1172 (2019), 012077.
[15] S.O. Aisida, I. Ahmad, F.I. Ezema, J. Phys. B: Condens. Matter 579 (2020), 411907.
[16] S.O. Aisida, I. Ahmad, T. Zhao, M. Maaza, F.I. Ezema, J. Macromol. Sci., Part B 59 (2020) 295–308.
[17] H. Zhao, H. Jia, S. Wang, D. Xue, Z. Zheng, J. Exper. Nanosci. 6 (2011) 75–83.
[18] X. Zhou, J. Liu, C. Wang, P. Sun, X. Hu, X. Li, K. Shimanoe, N. Yamazoe, G. Lu, Sens. Actuators, B 206 (2015) 577–583.

[19] Z. Jia, Q. Qin, J. Liu, X. Zhang, R. Hu, S. Li, R. Zhu, Superlattices Microstruct. 82 (2015) 174–187.
[20] M. Amiri, M. Salavati-Niasari, A. Akbari, Adv. Colloid Interface Sci. 265 (2019) 29–44.
[21] B.I. Kharisov, H.V.R. Dias, O.V. Kharisova, Arabian J. Chem. 12 (2019) 1234–1246.
[22] A.M. Lamukhin, G.A. Zinyagin, F.L. Skuridin, P.A. Kozlov, A.M. Panshin, V. G. Dyubanov, L.I. Leontyev, Ecol. Indust. Russ. 1 (2013) 4–7.
[23] A.A. Popov, G.V. Petrov, Proc. Irkutsk State Techn. Univ. (Vestnik Irkutskogo gosudarstvennogo tehnicheskogo universiteta) 4 (2016) 169–177.
[24] F.T. Lee, Miner. Process. Extract. Metall. 110 (2001) 14–24.
[25] F.T. Lee, J. Industr. Technol. 10 (2001) 59–83.
[26] C.-C. Wu, F.-C. Chang, W.-S. Chen, M.-S. Tsai, Y.-N. Wang, J. Environ. Management. 143 (2014) 208–213.
[27] R.N.C. De Siqueira, E.A. Brocchi, P.F. De Oliveira, M.S. Motta, Metall. Mater. Transact. 45 (2014) 66–75.
[28] N.M. Ivanova, E.A. Soboleva, Y.A. Visurkhanova, Z. Muldakhmetov, Russ. J. Electrochem. 56 (2020) 533–543.
[29] Y.A. Vissurkhanova, E.A. Soboleva, N.M. Ivanova, Z.M. Muldakhmetov, Bull. Karaganda State Univ. Chem. Ser. 2 (2020) 42–50.
[30] N.M. Ivanova, E.A. Soboleva, Y.A. Visurkhanova, Russ. Chem. Bull. 69 (2020) 1428–1435.